Kumtyubeite Ca$_5$(SiO$_4$)$_2$F$_2$—A new calcium mineral of the humite group from Northern Caucasus, Kabardino-Balkaria, Russia

Irina O. Galuskina,[1],* Biljana Lazic,[2] Thomas Armbruster,[2] Evgeny V. Galuskin,[1] Viktor M. Gazeev,[3] Aleksander E. Zadov,[4] Nikolai N. Pertsev,[3] Lidia Jeżak,[5] Roman Wrzalik,[6] and Anatoly G. Gurbanov[3]

[1]Faculty of Earth Sciences, Department of Geochemistry, Mineralogy and Petrography, University of Silesia, Będzińska 60, 41-200 Sosnowiec, Poland
[2]Mineralogical Crystallography, Institute of Geological Sciences, University of Bern, Freiestrasse 3, CH-3012 Bern, Switzerland
[3]Institute of Geology of Ore Deposits, Geochemistry, Mineralogy and Petrography (IGEM) RAS, Staromonetny 35, 119017 Moscow, Russia
[4]OOO NPP TEPLOCHIM, Dmitrovskoye av. 71, 127238 Moscow, Russia
[5]Institute of Geochemistry, Mineralogy and Petrology, University of Warsaw, al. Żwirki i Wigury 93, 02-089 Warszawa, Poland
[6]Institute of Physics, University of Silesia, Uniwersytecka 4, 40-007 Katowice, Poland

Abstract

Kumtyubeite, Ca$_5$(SiO$_4$)$_2$F$_2$—the fluorine analog of reinhardbraunsite with a chondrodite-type structure—is a rock-forming mineral found in skarn carbonate-xenoliths in ignimbrites of the Upper Chegem volcanic structure, Kabardino-Balkaria, Northern Caucasus, Russia. The new mineral occurs in spurrite-rondorfite-ellestadite zones of skarn. The empirical formula of kumtyubeite from the holotype sample is Ca$_5$(Si$_{1.99}$Ti$_{0.01}$)$_{\Sigma 2}$O$_8$(F$_{1.39}$OH$_{0.61}$)$_{\Sigma 2}$. Single-crystal X-ray data were collected for a grain of Ca$_5$(SiO$_4$)$_2$(F$_{1.3}$OH$_{0.7}$) composition, and the structure refinement, including a partially occupied H position, converged to $R = 1.56\%$: monoclinic, space group $P2_1/a$, $Z = 2$, $a = 11.44637(18)$, $b = 5.05135(8)$, $c = 8.85234(13)$ Å, $\beta = 108.8625(7)°$, $V = 484.352(13)$ Å^3. For direct comparison, the structure of reinhardbraunsite Ca$_5$(SiO$_4$)$_2$(OH$_{1.3}$F$_{0.7}$) from the same locality has also been refined to $R = 1.9\%$, and both symmetry independent, partially occupied H sites were determined: space group $P2_1/a$, $Z = 2$, $a = 11.4542(2)$, $b = 5.06180(10)$, $c = 8.89170(10)$ Å, $\beta = 108.7698(9)°$, $V = 488.114(14)$ Å^3. The following main absorption bands were observed in kumtyubeite FTIR spectra (cm^{-1}): 427, 507, 530, 561, 638, 779, 865, 934, 1113, and 3551. Raman spectra are characterized by the following strong bands (cm^{-1}) at: 281, 323, 397 (v_2), 547 (v_4), 822 (v_1), 849 (v_1), 901 (v_3), 925 (v_3), 3553 (v_{OH}). Kumtyubeite with compositions between Ca$_5$(SiO$_4$)$_2$F$_2$ and Ca$_5$(SiO$_4$)$_2$(OH$_{1.0}$F$_{1.0}$) has only the hydrogen bond O5-H1···F5′, whereas reinhardbraunsite with compositions between Ca$_5$(SiO$_4$)$_2$(OH$_{1.0}$F$_{1.0}$) and Ca$_5$(SiO$_4$)$_2$(OH)$_2$ has the following hydrogen bonds: O5-H1···F5′, O5-H1···O5′, and O5-H2···O2.

Keywords: Kumtyubeite, new mineral, reinhardbraunsite, crystal structure, chondrodite, composition, Raman, FTIR, Northern Caucasus, Russia

Introduction

Kumtyubeite, Ca$_5$(SiO$_4$)$_2$F$_2$, the calcium analog of chondrodite, was discovered in contact-metasomatic rocks formed by interaction of carbonate xenoliths with subvolcanic magma and volcanites of the Upper Chegem caldera structure, Kabardino-Balkaria, Northern Caucasus, Russia (Gazeev et al. 2006). Kumtyubeite is the fluorine analog of reinhardbraunsite, Ca$_5$(SiO$_4$)$_2$(OH)$_2$. Reinhardbraunsite (Karimova et al. 2008) and Ca$_7$(SiO$_4$)$_3$(OH)$_2$ (IMA2008-38, Galuskin et al. in preparation), the Ca and hydroxyl analog of humite, were also discovered in the same xenoliths.

Minerals belonging to the humite group are characterized by the crystal-chemical formula nA$_2$SiO$_4 \times$ A(F,OH)$_2$, where A = Mg, Fe^{2+}, Mn^{2+}, Zn, Ca, and others with n = 1, 2, 3, or 4. The humite group of minerals, sensu stricto, comprises nesosilicates with cations in octahedral sites and additional (OH)$^-$, F$^-$ groups

(Jones et al. 1969; Ribbe and Gibbs 1971). From a structural point of view (Thompson 1978), they are polysomes assembled of norbergite and olivine modules. Strunz and Nickel (2001) classify the corresponding minerals as norbergite-chondrodite group distinct from the ribbeite-leucophoenicite-jerrygibbsite group, which may also be derived by the same crystal-chemical formula given above but the M(O,OH)$_6$ chains are linked by dimers of edge-sharing SiO$_4$ tetrahedra with only one Si site of the dimer being statistically occupied.

Among minerals, hydroxyl analogs of the humite group seem to predominate. Only in case of Mg end-members does a complete polysomatic series of F-dominant phases exist: norbergite Mg$_3$(SiO$_4$)(F,OH), chondrodite (Mg,Fe^{2+})$_5$(SiO$_4$)$_2$(F,OH)$_2$, humite (Mg,Fe^{2+})$_7$(SiO$_4$)$_3$(F,OH)$_2$, and clinohumite (Mg,Fe^{2+})$_9$(SiO$_4$)$_4$(F,OH), whereas only one hydroxyl analog of the Mg end-members is known: hydroxyl-clinohumite (Gekimyants et al. 1999). Within the chondrodite series three mineral species have been defined up to now: alleghanyite Mn$_5$(SiO$_4$)$_2$(OH)$_2$, chondrodite (Mg,Fe^{2+})$_5$(SiO$_4$)$_2$(F,OH)$_2$,

* E-mail: irina.galuskina@us.edu.pl

and reinhardbraunsite $Ca_5(SiO_4)_2(OH,F)_2$.

Reinhardbraunsite was discovered in altered xenoliths within volcanic rocks of Eifel, Germany (Hamm and Hentschel 1983; Kirfel et al. 1983); later it was described in pyrometamorphic rocks of Hatrurim, Negev, Israel (Sokol et al. 2007). Analytical data of alleged high-F reinhardbraunsite were presented from carbonatites of Fort Portal, Uganda (Barker and Nixon 1989), but the low total and the significant Na content cast some doubts on its identity. Analogs of kumtyubeite were found in burned coal dumps at Kopeisk, Southern Ural, Russia (Chesnokov et al. 1993). In addition, the phase $Ca_5(SiO_4)_2F_2$, usually reported as $2C_2S \cdot CaF_2$, is a component of cement clinker (Gutt and Osborne 1966; Taylor 1997; Watanabe et al. 2002). Gutt and Osborne (1966) also published approximate cell dimensions and optical data for the synthetic product indicating identity with kumtyubeite.

Kumtyubeite $Ca_5(SiO_4)_2F_2$ was approved as a new mineral species in December 2008 by the IMA-CNMNC. In this paper, composition, crystal structure, spectroscopy, and mineral association of this new mineral are reported. The name kumtyubeite derives from Kum-Tyube—the name of a mountain plateau situated at the locality where this mineral was found. Type material is deposited in the collection of the Museum of Natural History, Bern, specimen number NMBE 39572 and in the collection of the Fersman Mineralogical Museum, Moscow, specimen number 3732/1.

METHODS OF INVESTIGATION

Morphology and mineral association were investigated with a Philips XL 30 ESEM scanning electron microscope. Chemical analyses were carried out by means of a CAMECA SX-100 electron microprobe (WDS mode, 15 kV, 15 nA, 1–3 μm beam diameter). The following standards and lines were used: $TiK\alpha$ = rutile; $CaK\alpha$, $SiK\alpha$ = wollastonite, diopside; $MgK\alpha$ = diopside; $PK\alpha$ = apatite; $NaK\alpha$ = albite; $FeK\alpha$ = Fe_2O_3, andradite; $MnK\alpha$ = rhodonite; $ClK\alpha$ = tugtupite; $FK\alpha$ = synthetic fluorphlogopite; $CrK\alpha$ = synthetic Cr_2O_3; $SK\alpha$ = barite. Recommendations on fluorine measurements (Ottolini et al. 2000) in Mg-rich humites were taken into consideration. Corrections were calculated using the PAP procedures suggested by CAMECA.

An X-ray powder pattern of kumtyubeite was recorded using a Philips X'Pert PW 3710 powder diffractometer (filtered $CoK\alpha$-radiation, 45 kV, 30 mA, 0.01° step, 100 s/step).

The selection of the two crystals of reinhardbraunsite and kumtyubeite for structure refinement was solely based on crystal quality (low concentration of inclusions, sharp X-ray reflections). For this reason the crystals do not correspond to the most OH- or F-rich compositions determined from this locality. Single crystals of kumtyubeite $Ca_5(SiO_4)_2(F_{1.3}OH_{0.7})$ and reinhardbraunsite $Ca_5(SiO_4)_2(OH_{1.3}F_{0.7})$ from the same locality were mounted on a Bruker Apex II three-circle CCD diffractometer using graphite monochromated $MoK\alpha$ X-radiation for diffraction intensity-data collection. Preliminary lattice parameters and an orientation matrix were obtained from three sets of frames and refined during the integration process of the intensity data. Diffraction data were collected with a combination of ω and φ scans (program SMART, Bruker 1999). Integrated intensities were obtained using the SAINT computer program (Bruker 1999). An empirical absorption correction using SADABS (Sheldrick 1996) was applied. Reflection statistics and systematic absences were consistent with space group $P2_1/a$ (no. 14) already known for reinhardbraunsite. The standard setting of this space group is $P2_1/c$ but in accordance with the refinement of reinhardbraunsite (Kirfel et al. 1983) the $P2_1/a$ setting was preferred. In addition, we used the same atom labeling scheme as Kirfel et al. (1983). Structural refinement was performed using SHELXL-97 (Sheldrick 1997). Scattering factors for neutral atoms were employed. Positions of the hydrogen atoms of the hydroxyl groups were derived from difference-Fourier syntheses. Subsequently, partially occupied hydrogen positions were refined at a fixed value of $U_{iso} = 0.05$ Å², and O-H distances were restrained to 0.95(2) Å. Data collection and refinement details are summarized in Table 1. CIF files are available online.[1]

IR spectra of kumtyubeite were obtained on a Bio-Rad FTS-6000 spectrophotometer with a micro-ATR accessory (MIRacle), equipped with KRS-5 lenses and a single-reflection diamond ATR. A small amount of sample was simply placed onto the ATR crystal. During analysis a pressure of up to 75 psi was applied to the sample. FTIR spectra (32 scans) were averaged to obtain background and sample spectra. Spectra were collected from 360 to 6000 cm⁻¹ with a resolution of 4 cm⁻¹.

Raman spectra of single crystals of kumtyubeite (20–30 μm) were recorded using a LabRam System spectrophotometer (Jobin-Yvone-Horiba), equipped with a grating monochromator, a charge-coupled device (CCD), a Peltier-cooled detector (1024 × 256) and an Olympus BX40 confocal microscope. The incident laser excitation was provided by a water-cooled argon laser source operating at 514.5 nm. The power at the exit of a 50× or 100× objective lens varied from 20 to 40 mW. To avoid undesirable Rayleigh scattering, two notch-filters were used, cutting the laser line at 200 cm⁻¹. Raman spectra were recorded at 0° geometry in the range 200–4000 cm⁻¹ with a resolution of 3.5 cm⁻¹. The monochromator was calibrated using the Raman scattering line of a silicon plate (520.7 cm⁻¹).

TABLE 1. Parameters for X-ray data collection and crystal-structure refinement of kumtyubeite and reinhardbraunsite

Crystal data	Kumtyubeite	Reinhardbraunsite
Unit-cell dimensions (Å)*	$a = 11.44637(18)$	$a = 11.4542(2)$
	$b = 5.05135(8)$	$b = 5.06180(10)$
	$c = 8.85234(13)$	$c = 8.89170(10)$
	$\beta = 108.8625(7)°$	$\beta = 108.7698(9)°$
Volume (Å³)	484.352(13)	488.114(14)
Space group	$P2_1/a$ (no. 14)	$P2_1/a$ (no. 14)
Z	2	2
Chemical formula	$Ca_5(SiO_4)_2(OH_{0.7}F_{1.3})$	$Ca_5(SiO_4)_2(OH_{1.3}F_{0.7})$
μ (mm⁻¹)	3.06	3.03
Intensity measurement		
Crystal shape	prism	prism
Crystal size (mm)	$0.100 \times 0.060 \times 0.040$	$0.080 \times 0.060 \times 0.015$
Diffractometer	APEX II SMART	APEX II SMART
X-ray radiation	$MoK\alpha$, λ=0.71073 Å	$MoK\alpha$, λ=0.71073 Å
X-ray power	50 kV, 30 mA	50 kV, 30 mA
Monochromator	graphite	graphite
Temperature	293 K	293 K
Detector to sample distance	5.95 cm	3.95 cm
Measurement method	phi, omega scans	phi, omega scans
Rotation width	0.5°	0.5°
Total number of frames	1366	1746
Frame size	512×512 pixels	512×512 pixels
Time per frame	20 s	45 s
Max. θ-range for data collection	28.25	29.98
Index ranges	$-14 \leq h \leq 15$	$-16 \leq h \leq 15$
	$-6 \leq k \leq 5$	$-7 \leq k \leq 7$
	$-11 \leq l \leq 11$	$-12 \leq l \leq 12$
No. of measured reflections	6905	9218
No. of unique reflections	1202	1419
No. of observed reflections [$I > 2\sigma(I)$]	1153	1249
Refinement of the structure		
No. of parameters used in refinement	81	85
R_{int}	0.0231	0.0350
R_σ	0.0139	0.0224
$R1, I > 2\sigma(I)$	0.0156	0.0190
$R1$, all data	0.0163	0.0236
$wR2$ (on F^2)	0.0444	0.046
GooF	1.103	1.115
$\Delta\rho_{min}$ (–e Å⁻³)	–0.27 close to Si1	–0.33 close to H1
$\Delta\rho_{max}$ (e Å⁻³)	0.50 close to F	0.33 close to O1

* Based on 5305 (kumtyubeite) and 3987 reflections (reinhardbraunsite); the low e.s.d. values are probably not realistic but are a consequence of the high number of reflections applied.

OCCURRENCE, MINERAL ASSOCIATION, AND RESULTS OF KUMTYUBEITE INVESTIGATIONS

Kumtyubeite was discovered in xenolith 1 located between Lakargi and Vorlan mountain peaks within the Upper Chegem volcanic structure (xenolith numbering after Gazeev et al. 2006). The exposure of xenolith 1 reaches 20–25 m² (Gazeev et al. 2006). Its central part is composed of bluish-gray marble with banding relics. Massive dark gray spurrite-calcite rocks encase the marble core. Some small xenolith outcrops (1–1.5 m across) occur along the west and northwest contacts of xenolith 1. They are light colored from white to yellow or red and contain abundant calcium minerals of the humite group: $Ca_7(SiO_4)_3(OH)_2$, and reinhardbraunsite or kumtyubeite.

More rarely, small fragments of light spurrite rocks, 50 cm in size, with striking pink spots of reinhardbraunsite and yellow oval rondorfite patches are noted. At the contact of xenolith with ignimbrites, cuspidine rocks with larnite, rondorfite, rustumite, and wadalite are developed.

Reinhardbraunsite, the new mineral $Ca_7(SiO_4)_3(OH)_2$, ron-dorfite, P- and As-bearing ellestadite-(OH), wadalite, Sn- and U-bearing lakargiite, srebrodolskite, and magnesioferrite are commonly distributed in different types of skarn rocks. Per-ovskite, ferrigarnet of kimzeyite type, periclase, and sphalerite are considerably less abundant. Secondary calcium hydrosilicates (bultfonteinite, hillebrandite, afwillite), minerals of the ettringite group, hydrocalumite, hydrogarnets, calcite, and brucite are fairly common.

Kumtyubeite is noted in spurrite-rondorfite-ellestadite zones of skarn, developed along the west contact of the xenolith (Figs. 1a–1c). In hand specimens of the grayish-reddish matrix, kum-tyubeite forms oval spots up to 1 cm across, composed of light-pink grains 250 μm in maximum dimension. Kumtyubeite of the holotype specimen has an invariable composition corresponding to $Ca_5(Si_{1.99}Ti_{0.01})_{\Sigma2}O_8(F_{1.39}OH_{0.61})_{\Sigma2}$ (Table 2; analysis 1). The kumtyubeite composition in rocks enriched in bultfonteinite (Table 2; analysis 12) is very similar: $Ca_{5.01}(Si_{1.98}Ti_{0.01})_{\Sigma1.99}O_8$ $(F_{1.36}OH_{0.62})_{\Sigma1.98}$ (Table 2, analysis 2). Kumtyubeite contains inclusions of the potential new mineral "Ca-humite" $Ca_7(SiO_4)_3F_2$, rondorfite, rarely lakargiite and kimzeyite (Figs. 1a–1b). If
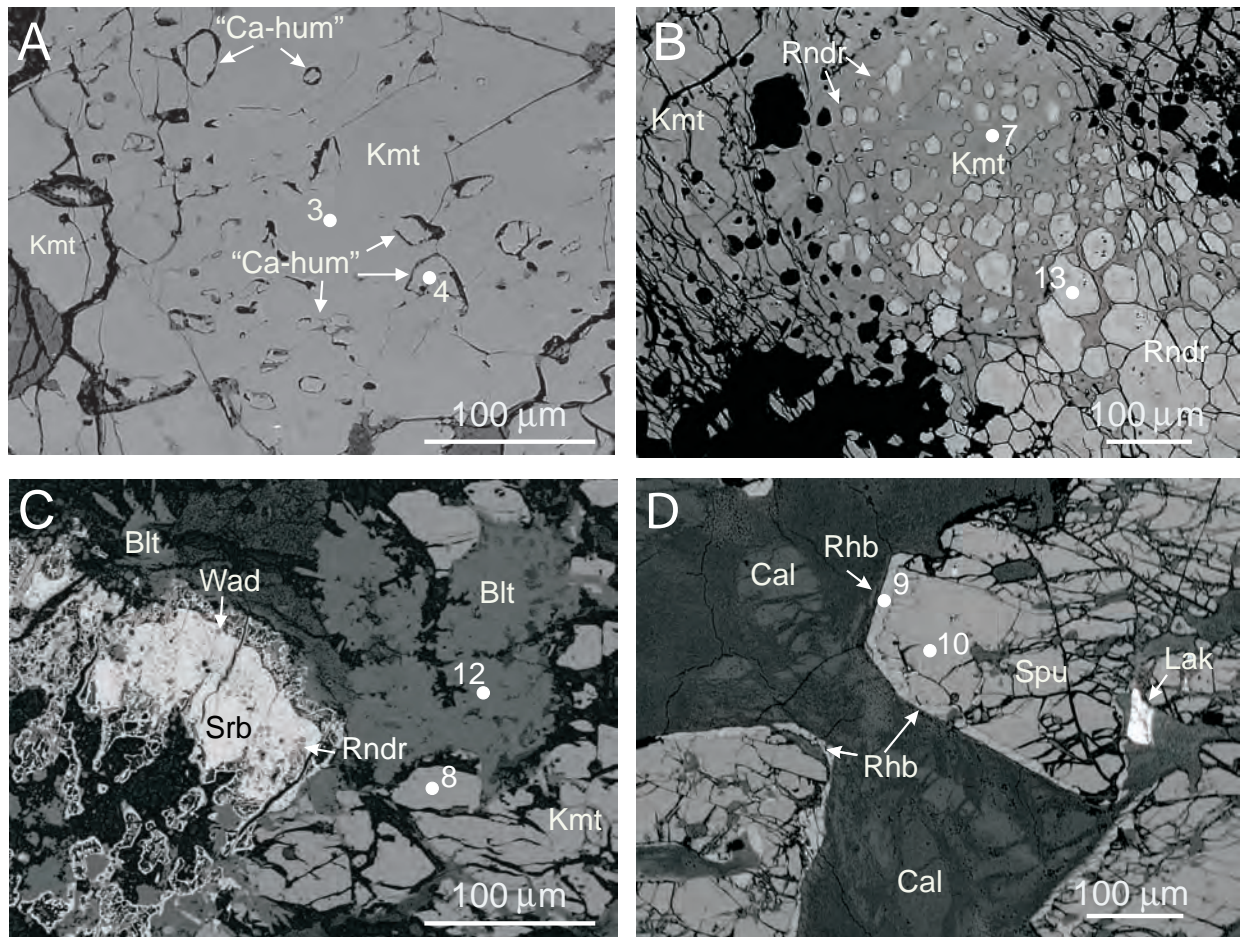
FIGURE 1. A = kumtyubeite grain with "Ca-humite" inclusions; B = kumtyubeite with rounded rondorfite inclusions, black spots = products of rondorfite alteration, Ca-hydrosilicates; C = kumtyubeite associated with srebrodolskite, bultfonteinite, and Ca-hydrosilicates, and ettringite (dark gray); D = reinhardbraunsite substituting for spurrite along the rims of spurrite grains; numbers correspond to the number of analyses in Table 1. Blt = bultfonteinite, "Ca-hum" = "Ca-humite," Cal = calcite, Kmt = kumtyubeite, Lak = lakargiite, Rndr = rondorfite, Spu = spurrite, Srb = srebrodolskite, Wad = wadalite.

TABLE 2. Chemical composition (wt%) of kumtyubeite and associated minerals

	1			2			3	4	5	6	7	8	9	10	11	12	13
	mean 28	SD	range	mean 29	SD	range											
SO_3	n.d.			n.d.			n.d.	n.d.	n.d.	n.d.	n.d.	0.07	n.d.	0.05	n.d.	0.69	n.d.
P_2O_5	n.d.			n.d.			n.d.	n.d.	n.d.	n.d.	n.d.	n.d.	n.d.	n.d.	n.d.	n.d.	0.19
TiO_2	0.09	0.07	0–0.29	0.10	0.06	0.02–0.25	0.27	0.10	0.20	0.14	0.23	0.41	0.05	n.d.	0.18	0.05	n.d.
SiO_2	28.20	0.15	27.85–28.54	28.02	0.17	27.71–28.38	27.92	29.94	27.86	30.02	27.94	27.91	28.54	26.98	28.21	27.20	29.99
Al_2O_3	n.d.			n.d.			n.d.	n.d.	n.d.	n.d.	n.d.	n.d.	n.d.	n.d.	n.d.	0.02	0.13
Fe_2O_3	0.04	0.05	0–0.29	0.02	0.03	0–0.11	n.d.	n.d.	0.02	n.d.	n.d.	n.d.	n.d.	n.d.	n.d.	0.10	0.08
Cr_2O_3	n.d.			n.d.			n.d.	n.d.	0.05	n.d.	n.d.	n.d.	n.d.	n.d.	n.d.	n.d.	0.02
CaO	66.19	0.68	64.51–67.26	66.38	0.29	65.46–66.88	65.78	65.47	66.42	65.99	66.08	66.23	66.74	62.97	66.27	53.36	56.50
MgO	0.05	0.02	0–0.09	0.04	0.02	0.01–0.08	0.05	0.03	0.03	0.03	0.05	0.03	n.d.	n.d.	n.d.	n.d.	4.63
MnO	n.d.			0.03	0.04	0–0.13	n.d.	0.07	0.02	n.d.	n.d.	0.02	n.d.	n.d.	n.d.	n.d.	n.d.
Na_2O	n.d.			n.d.			n.d.										0.04
F	6.22	0.32	5.54–6.73	6.09	0.36	5.42–6.77	6.25	4.22	5.26	3.68	6.46	5.78	4.24	n.d.	1.72	8.63	n.d.
Cl	n.d.			0.03	0.02	0–0.05	n.d.	n.d.	0.04	n.d.	n.d.	0.04	n.d.	n.d.	n.d.	n.d.	8.72
H_2O†	1.25			1.33	0.17	1.02–1.67	1.30	1.02	0.88	1.22	1.19	1.48	2.14	n.d.	3.41	12.98	
$-O \equiv F + Cl$	2.64			2.56			2.65	1.79	2.23	1.55	2.74	2.44	1.80			3.66	1.94
Total	99.40			99.48			98.92	99.11	98.50	99.53	99.21	99.53	99.91	99.90*	99.06	99.37	98.36
Na																0.01	
Ca	5.00			5.01			5	6.99	5.00	7.01	5.01	5	5	5	5	2.02	8.03
Mn^{2+}								0.01									
Mg																	0.92
X	**5**			**5.01**			**5**	**7**	**5**	**7.01**	**5.01**	**5**	**5**	**5**	**5**	**2.02**	
Si	1.99			1.98			1.98	2.99	1.98	2.98	1.98	1.98	2	2	1.99	0.96	3.98
Ti^{4+}	0.01			0.01			0.01	0.01	0.01	0.01	0.01	0.02			0.01		
Fe^{3+}																	0.01
Al																	0.02
P																	0.02
S^{6+}																0.02	
Z	**2.00**			**1.99**			**1.99**	**3**	**1.99**	**2.99**	**1.99**	**2**	**2**	**2**	**2**	**0.98**	
F	1.39			1.36			1.40	1.33	1.17	1.16	1.45	1.29	0.94		0.39	0.97	
OH	0.60			0.62			0.60	0.67	0.83	0.82	0.55	0.71	1.06		1.61	3.03	
Cl																	1.96
C														1			

Notes: 1 = analyses of holotype kumtyubeite; 2 = kumtyubeite from bultfonteinite-bearing rock; 3–6 = kumtyubeite grain (3,5) with inclusions of "Ca-humite" (4,6); 7 = kumtyubeite with rondorfite inclusions (13); 8 = kumtyubeite with srebrodolskite and bultfonteinite (12); 9 = reinhardbraunsite rim on spurrite (10); 10 = reinhardbraunsite associated with "Ca-OH-humite." The sums of cations on the octahedral X and the tetrahedral Z sites are printed in bold.
* CO_2 = 9.90 wt% in total.
† Calculated on the basis of charge balance. Kumtyubeite and reinhardbraunsite analyses were normalized on 7 cations, "Ca-humites" were normalized on 10 cations, bultfonteinite was normalized on 3 cations, rondorfite on 13 cations.

replaced by kumtyubeite, relic "Ca-humite" $Ca_7(SiO_4)_3F_2$ is preserved as lentil-like, elongated inclusions, the boundary of which is sometimes transformed to secondary hydrosilicates (Fig. 1a). It is interesting that in the case of partial replacement, the F/OH ratio in newly formed kumtyubeite is more or less the same as in primary "Ca-humite" (Table 2, analyses 3–6). Rondorfite is also characteristically found in this association, occurring as rounded, isometric inclusions in kumtyubeite, partly replaced by calcium hydrosilicates (Fig. 1b; Table 2, analyses 7 and 13). P- and As-bearing ellestadite-(OH) associated with kumtyubeite is often replaced by minerals of the ettringite and hydrogarnet groups.

Srebrodolskite and magnesioferrite, forming aggregates reaching 500 μm in size, and also ferrigarnet of kimzeyite type, wadalite, and sphalerite are accessory minerals. Representative analyses of srebrodolskite, magnesioferrite, and lakargiite are given in Table 3. Kumtyubeite associated with srebrodolskite is characterized by increased Ti content (Fig. 1c; Table 2, analysis 8).

Reinhardbraunsite is confined to spurrite zones of the skarn, which change to kumtyubeite-spurrite-rondorfite-ellestadite zones toward the xenolith center. Kumtyubeite appears predominantly replacing $Ca_7(SiO_4)_3F_2$, whereas reinhardbraunsite replaces spurrite and $Ca_7(SiO_4)_3(OH)_2$ (Fig. 1d). It is interesting that larnite relics are absent within kumtyubeite and reinhardbraunsite, whereas these relics are characteristic of

$Ca_7(SiO_4)_3(OH)_2$ (Galuskin et al. in preparation). $Ca_7(SiO_4)_3(OH)_2$ coexists with reinhardbraunsite having low fluorine content (Table 2, analysis 11).

Kumtyubeite shows vitreous luster and is transparent. The mean Moh's hardness is 5–6, the mean measured micro-hardness VHN_{50} = 300 (280–320) kg/mm² (11 measurements), the mineral is brittle, the cleavage is distinct on (001), in particular for crystals with a ratio OH:F ≈ 1.

Kumtyubeite is transparent and colorless in thin-section. It is biaxial negative, with n_α = 1.594(2), n_β = 1.605(2), n_γ = 1.608(2), δ = 0.014, $2V_X$ (meas.) = 40–55°, $2V_X$ (calc.) = 54.8°, $X \wedge c$ = 15(2)°, Z = b. Simple, rarely polysynthetic, twins on (001) are characteristic for kumtyubeite. D_{calc} is 2.866 g/cm³.

Numerous inclusions in kumtyubeite did not permit selection of a pure fraction for a powder X-ray diffraction investigation using a Philips X'Pert PW 3710 powder diffractometer (Co$K\alpha$ radiation). The collected pattern contained strong peaks for "Ca-humite," ettringite and weak peaks for hydrogrossular, spurrite, wadalite-mayenite, hydrocalumite, and other phases. Nevertheless, we were able to extract the strongest peaks of the kumtyubeite pattern (Table 4) and to refine cell parameters. The PowderCell for Windows version 2.4 program (Kraus and Nolze 1996), based on the Rietveld method, was used to refine lattice parameters (R =13). Starting parameters were taken from the single-crystal data of kumtyubeite. Refined cell dimensions from

TABLE 3. Chemical composition of oxides associated with kumtyubeite

|	1	2	3
UO_3 wt%	n.m.	n.m.	4.25
Nb_2O_5	n.d.	n.d.	0.95
TiO_2	0.35	0.55	10.53
ZrO_2	n.m.	0.08	42.24
SiO_2	0.11	0.01	0.01
HfO_2	n.m.	n.d.	0.93
ThO_2	n.m.	n.m.	0.31
SnO_2	n.d.	n.d.	5.62
MnO_2	n.d.	1.36	n.d.
Fe_2O_3	71.80	48.99	3.13
Al_2O_3	1.49	4.04	n.d.
V_2O_3	0.05	n.d.	n.d.
Sc_2O_3	n.m.	n.m.	0.23
Cr_2O_3	n.d.	0.06	0.07
La_2O_3	n.m.	n.m.	0.15
Ce_2O_3	n.m.	n.m.	0.33
CaO	0.80	41.79	32.42
MgO	9.79	0.20	0.02
FeO	2.09		
MnO	11.74	1.94	n.d.
ZnO	1.20	n.m.	n.m.
SrO	n.m.	n.m.	0.22
Total	99.42	99.02	101.41
Ca	0.031	2.001	0.991
Mg	0.519		0.001
Mn^{2+}	0.354		
Sr			0.003
Fe^{2+}	0.063		
Zn	0.032		
Ce^{3+}			0.003
La^{3+}			0.002
Th			0.002
X	*0.999*	*2.001*	*1.002*
Fe^{3+}	1.924	1.647	0.067
Al	0.063	0.213	
Mn^{4+}		0.042	
Mn^{2+}		0.073	
Mg		0.001	
Si	0.004	0.001	
Ti^{4+}	0.009	0.019	0.226
Zr		0.002	0.588
Sn			0.064
Sc			0.006
U^{6+}			0.026
Cr		0.002	0.002
Nb^{5+}			0.012
Hf			0.008
Y	*2.000*	*2.000*	*0.999*

Note: 1 = magnesioferrite, normalized on 3 cations; 2 = srebrodolskite, normalized on 4 cations; 3 = lakargiite, normalized on 2 cations; n.m. = not measured; n.d. = not detected.

TABLE 4. X-ray powder diffraction data (d in angstroms) of kumtyubeite

hkl	Measured d (Å)	I	Calculated d (Å)	I	hkl	Measured d (Å)	I	Calculated d (Å)	I
001	8.3830	1	8.4083	8	$22\bar{2}$	2.1369	3	2.1369	7
200	5.4202	30	5.4215	33	$51\bar{2}$	2.0511	2	2.0514	5
110	4.5824	1	4.5859	2	$11\bar{4}$	2.0126	4	2.0125	11
$01\bar{1}$	4.3297	3	4.3319	10	510	1.9926	3	1.9929	7
002	4.1915	3	4.1948	7	$01\bar{4}$	1.9360	2	1.9352	2
201	4.0006	4	4.0003	14	$51\bar{3}$	1.9128	2	1.9123	2
111	3.8081	13	3.8102	34	222	1.9040	100	1.9043	100
210	3.6973	5	3.6987	10	$42\bar{1}$	1.8952	37	1.8955	45
$11\bar{2}$	3.3273	21	3.3274	55	023	1.8748	2	1.8751	5
$01\bar{2}$	3.2269	4	3.2281	4	511	1.8209	4	1.8208	13
211	3.1374	3	3.1384	5	114	1.8145	2	1.8151	1
$31\bar{1}$	3.0344	37	3.0340	78	$60\bar{3}$	1.8063	14	1.8064	22
310	2.9399	17	2.9410	45	313	1.8027	23	1.8029	28
112	2.9018	16	2.9016	67	$42\bar{3}$	1.7267	3	1.7266	11
$20\bar{3}$	2.8932	13	2.8942	59	$51\bar{4}$	1.7216	6	1.7218	14
$40\bar{1}$	2.8635	3	2.8639	5	403	1.6915	4	1.6915	17
003	2.7943	2	2.7959	8	005	1.6766	9	1.6765	34
$31\bar{2}$	2.7737	25	2.7744	60	$60\bar{4}$	1.6587	28	1.6588	39
400	2.7101	12	2.7103	18	$13\bar{1}$	1.6492	3	1.6492	7
311	2.5713	20	2.5718	32	131	1.6183	2	1.6181	8
$11\bar{3}$	2.5452	12	2.5463	40	$13\bar{2}$	1.5748	2	1.5747	4
020	2.5282	2	2.5276	8	$71\bar{2}$	1.5551	6	1.5551	25
$21\bar{3}$	2.5112	17	2.5115	33	$33\bar{1}$	1.5403	8	1.5402	6
$41\bar{1}$	2.4917	10	2.4922	26	314	1.5274	2	1.5273	8
120	2.4621	2	2.4637	14	132	1.5221	1	1.5220	5
$40\bar{3}$	2.3640	2	2.3642	7	$33\bar{2}$	1.5026	2	1.5027	5
121	2.3168	2	2.3171	6	$60\bar{5}$	1.4925	4	1.4924	7
113	2.2530	2	2.2539	6					
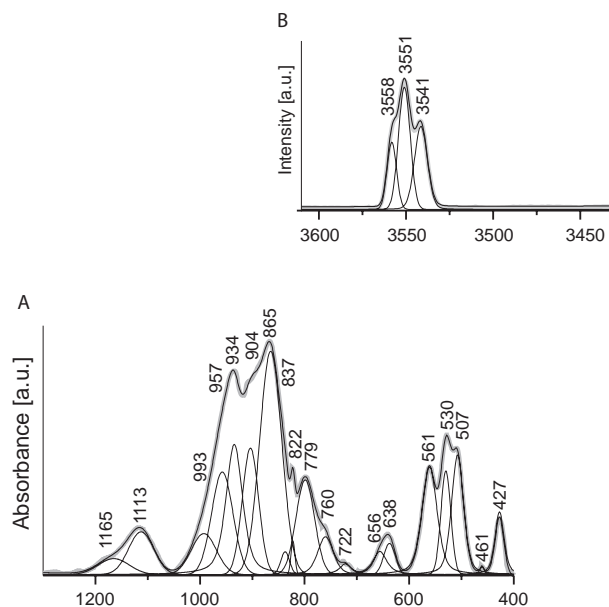
FIGURE 2. FTIR spectra of a kumtyubeite grain measured with micro-ATR accessory in the region: A = 1250–400 cm^{-1}, B = 3600–3450 cm^{-1}.

the powder data are given below: monoclinic, space group: $P2_1/a$, $a = 11.454(2)$, $b = 5.056(1)$, $c = 8.857(1)$ Å, $\beta = 108.84(1)°$, $V = 485.51(2)$ Å^3, $Z = 2$.

FTIR and Raman spectra of kumtyubeite resemble spectra of humite-group minerals (Prasad and Sarma 2004; Frost et al. 2007a, 2007b). The FTIR spectrum of kumtyubeite shows the following bands (main bands are italic): *427*, *507*, *530*, *561*, *638*, 656, 722, 760, *779*, 822, 837, *865*, 904, *934*, 957, 993, *1113*, 1165, 3541, *3551*, and 3558 cm^{-1} (Fig. 2). The following bands appear in the Raman spectrum of kumtyubeite (strong bands are italic): *281*, 299, *323*, *397*, 420, 525, *547*, 822, *849*, 901, *925*, 3544, *3553*, and 3561 cm^{-1} (Fig. 3). In the low-frequency (<1000 cm^{-1}) region, the Raman spectra of kumtyubeite and reinhardbraunsite of xenolith 1 (Fig. 3) strongly resemble each other. FTIR and Raman bands measured for the reinhardbraunsite–kumtyubeite series may be divided into four groups following Frost et al. (2007a,

2007b): group 1 = modes lower than 400 cm^{-1} corresponding to the vibrations of CaO$_6$ octahedra; group 2 = modes 400–700 cm^{-1} are related to bending vibrations of SiO$_4$ tetrahedra; group 3 = modes 700–1000 cm^{-1} are related to the stretching vibrations of SiO$_4$; and group 4 = modes between 3480 and 3562 cm^{-1} are characteristic of (OH)-group vibrations.

The main difference between the reinhardbraunsite and kumtyubeite spectra consists in the absence of a strong band near 3480 cm^{-1} in the kumtyubeite spectrum. In addition, the intensity
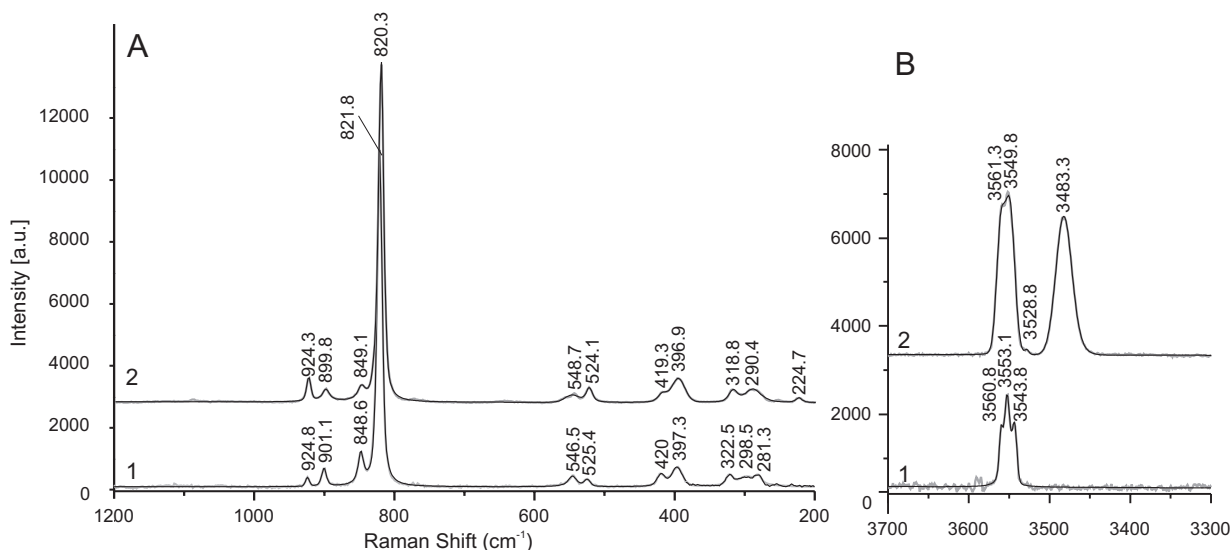
FIGURE 3. Raman spectra of kumtyubeite (1) and reinhardbraunsite (2) in the region: A = 1200–200 cm^{-1}, B = 3700–3300 cm^{-1}.
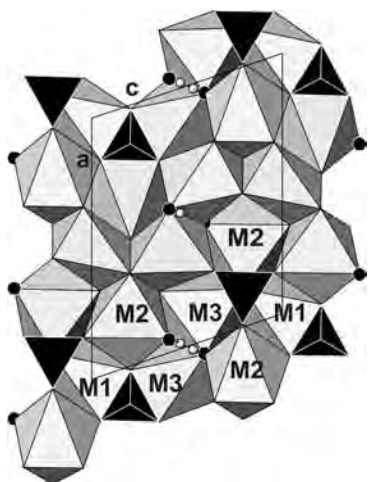

FIGURE 4. [010] projection of the polyhedral structure model of kumtyubeite. Three symmetry independent CaO$_6$ octahedra are labeled M1 to M3; the SiO$_4$ tetrahedron is black with light gray outlines; (OH,F) sites are indicated by black circles with white rim. Disordered H1 is shown as small gray sphere.

FIGURE 5. Disordered hydrogen-bond system in reinhardbraunsite solid-solution members with compositions between Ca$_5$(SiO$_4$)$_2$(OH)$_2$ and Ca$_5$(SiO$_4$)$_2$(OH)F: SiO$_4$ tetrahedra are represented by dark polyhedra, bonds are drawn for Ca-O and O-H, dashed lines indicate O···H acceptor interactions. The two opposite structural fragments are related to each other by an inversion center between H1 and H1'. The sub-site F5 centers a triangle formed by 2 × Ca3 and 1 × Ca2, whereas the sub-site O5 is shifted toward the symmetry center. H1 is at maximum 50% occupied avoiding short H1-H1' distances. In kumtyubeite solid-solution members with compositions between Ca$_5$(SiO$_4$)$_2$(F)$_2$ and Ca$_5$(SiO$_4$)$_2$F(OH), H2 is empty.

of the band near 3550 cm^{-1} (Figs. 2 and 3) is also weaker in kumtyubeite than in reinhardbraunsite. The two main bands are related to the hydrogen sites H1 and H2. In kumtyubeite, which is characterized by high F content, the H2 site is not occupied (see single-crystal structure investigations below). At this point one may easily be misled by assuming that the 3480 cm^{-1} absorption is caused by the hydrogen bond related to H2. However, as shown below, the situation is much more complex.

SINGLE-CRYSTAL STRUCTURAL INVESTIGATION OF KUMTYUBEITE AND REINHARDBRAUNSITE

The crystal structures of kumtyubeite and reinhardbraunsite (Figs. 4 and 5; Tables 1 and 5–7) correspond to the chondrodite structure-type (Kirfel et al. 1983). A projection of a polyhedral structure model of kumtyubeite along [010] (Fig. 4) is indis-
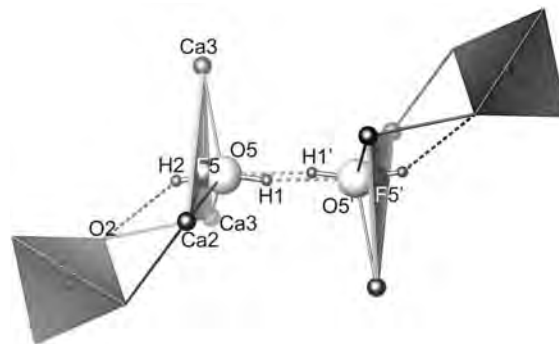
tinguishable from a corresponding drawing for chondrodite (Gibbs et al. 1970), with the only obvious difference being that the cell volume of kumtyubeite is ca. 26% greater than that of chondrodite due to the difference in octahedral ionic radii, 0.72 Å for Mg vs. 1.00 Å for Ca (Shannon 1976).

The reinhardbraunsite-kumtyubeite series is characterized by an increase in the unit-cell volume from the F end-member toward the OH end-member (Hamm and Hentchel 1983). This relation is also evident from this single-crystal X-ray study (Table 1), with the advantage that using the same equipment and data collection strategy for both crystals reduces systematic errors. There are already several structure refinements of reinhardbraunsite (Kirfel et al. 1983; Karimova et al. 2008) and its synthetic analog (Ganiev et al. 1969; Kuznetsova et al. 1980), but the quality of these previous studies was not sufficient to extract H sites

and to discuss the structural differences with kumtyubeite.

A special structural feature of solid-solution members between kumtyubeite and reinhardbraunsite is the strongly anisotropic smearing of O5 related to positional and chemical disorder. O5 is occupied by OH and by F. This average O5/F5 site lies on a triangular plane with $2 \times$ Ca3 and $1 \times$ Ca2 at the corners, and the disorder is most pronounced perpendicular to this plane. In the $Ca_5(SiO_4)_2(OH)_2$, end-member reinhardbraunsite, O5 acts simultaneously as donor and acceptor of a hydrogen bond. The reinhardbraunsite/kumtyubeite structure has a center of inversion halfway between two adjacent O5/F5 sites (Fig. 5). Thus, on a statistical basis, H1 between the two O5 sites can only be 50% occupied (Fig. 5). If both H1 sites were to be occupied (H1 occupancy = 100%), the two centrosymmetric H1 counterparts would be too close. For stoichiometric reasons, the reinhardbraunsite OH end-member must have 2 OH pfu. However, with H1 50%

occupied, it only contributes to 1 OH pfu. If O5 (Fig. 5) acts as acceptor of a hydrogen bond from O5′ (O5′-H1′⋯O5), O5 will also be hydroxylated but the alternate O5-H2 vector points almost opposite to the weak O5⋯H1 interaction (Fig. 5). This additional hydrogen bond system can be described as O5-H2⋯O2 (Fig. 5). Disordered hydrogen bonds are characteristic of the OH end-members of all humite-group minerals, as has been confirmed by neutron powder diffraction for synthetic hydroxylclinohumite (Berry and James 2001) and "hydroxyl-chondrodite" (Lager et al. 2001; Berry and James 2002).

The good quality of our diffraction data for the two solid-solution members invited splitting of the smeared O5 position into two sub-sites (O5 and F5). Subsequently, a refinement was done with individual O5 and F5 sites having a common isotropic displacement parameter and a constraint that the occupancies of both sub-sites sum to 1. Such a sub-site refinement involves one parameter less than the anisotropic O5 model. In the O5/F5 sub-site model for reinhardbraunsite, O5 and F5 are separated by 0.38 Å, whereas the corresponding distance in kumtyubeite is only 0.29 Å. In the case of reinhardbraunsite, we also refined F5/O5 populations and the occupancies agreed with values from the chemical analyses. A corresponding refinement for kumtyubeite was not so successful, probably because of the shorter O5-F5 distance, leading to strong overlap of the corresponding electron clouds. Thus, O5 and F5 occupancies were fixed to the value obtained from electron-microprobe analyses.

In reinhardbraunsite and kumtyubeite, F5 is on the plane formed by the triangle with $2 \times$ Ca3 and $1 \times$ Ca2 at the apices, whereas O5 is displaced from the triangular plane and shifted toward the symmetry center (Fig. 5). Thus, in accordance with the smaller ionic radius of F⁻ (1.30 Å) compared to O^{2-} (1.36 Å) for threefold coordination (Shannon 1976), corresponding distances between O5 and Ca are significantly longer than those between F5 and Ca (Table 7). A distance restraint [0.95(2) Å] between O5 and the two proton sites (H1 and H2) was applied to obtain physically meaningful O-H distances (Lager et al. 1987). The sub-site refinement for reinhardbraunsite yielded the following O⋯O distances for the various hydrogen-bond systems: O5-H1⋯O5′ 2.827 Å; O5-H1⋯F5′ 3.190 Å; O5-H2⋯O2 3.209 Å. According to the correlations between O-H stretching frequencies and O-H⋯O hydrogen bond lengths

TABLE 5a. Atomic coordinates and isotropic displacement parameters (U_{eq}) for kumtyubeite

Atom	Occup.	x	y	z	U_{eq} (Å²)
Ca1	1.0	1/2	0	1/2	0.00872(10)
Ca2	1.0	0.16958(2)	0.00430(5)	0.30946(3)	0.00788(9)
Ca3	1.0	0.38125(2)	0.00820(5)	0.07805(3)	0.00829(9)
Si1	1.0	0.35382(3)	0.57472(7)	0.29754(4)	0.00617(10)
O1	1.0	0.48464(8)	0.70458(17)	0.29303(10)	0.00864(18)
O2	1.0	0.24752(8)	0.70644(17)	0.14423(10)	0.00875(18)
O3	1.0	0.33001(8)	0.70447(17)	0.45559(10)	0.00855(18)
O4	1.0	0.35279(8)	0.25353(18)	0.29649(10)	0.00938(18)
O5	0.3	0.0466(4)	0.2161(9)	0.0743(5)	0.0130(2)
F5	0.7	0.05554(14)	0.2581(3)	0.09880(17)	0.0130(2)
H1	0.3	0.015(9)	0.052(11)	0.024(12)	0.050

TABLE 5b. Atomic coordinates and isotropic displacement parameters (U_{eq}) for reinhardbraunsite

Atom	Occup.	x	y	z	U_{eq} (Å²)
Ca1	1.0	1/2	0	1/2	0.00921(10)
Ca2	1.0	0.16976(3)	0.00251(6)	0.31087(4)	0.00875(8)
Ca3	1.0	0.38090(3)	0.00879(6)	0.07952(4)	0.00909(8)
Si1	1.0	0.35425(4)	0.57435(8)	0.29833(5)	0.00652(10)
O1	1.0	0.48447(10)	0.7052(2)	0.29332(12)	0.0087(2)
O2	1.0	0.24736(10)	0.7042(2)	0.14547(12)	0.0090(2)
O3	1.0	0.33012(10)	0.7043(2)	0.45581(12)	0.0090(2)
O4	1.0	0.35324(10)	0.2540(2)	0.29808(13)	0.0095(2)
O5	0.697(11)	0.0505(2)	0.2325(7)	0.0841(4)	0.0124(3)
F5	0.303(11)	0.0636(4)	0.2829(13)	0.1163(8)	0.0124(3)
H1	0.5	0.024(5)	0.080(8)	0.025(6)	0.050
H2	0.2	0.099(11)	0.36(2)	0.158(13)	0.050

TABLE 6a. Anisotropic displacement parameters U_{ij} (Å²) for kumtyubeite

Atom	U_{11}	U_{22}	U_{33}	U_{23}	U_{13}	U_{12}
Ca1	0.00913(18)	0.00746(18)	0.00819(17)	−0.00114(11)	0.00090(14)	−0.00112(11)
Ca2	0.00735(14)	0.00832(14)	0.00829(13)	−0.00020(8)	0.00295(10)	0.00047(8)
Ca3	0.00878(14)	0.00876(15)	0.00740(13)	0.00086(8)	0.00269(10)	−0.00004(8)
Si1	0.00674(16)	0.00521(17)	0.00647(16)	−0.00006(11)	0.00201(12)	0.00006(11)
O1	0.0075(4)	0.0088(4)	0.0098(4)	−0.0002(3)	0.0031(3)	−0.0001(3)
O2	0.0086(4)	0.0087(4)	0.0078(4)	0.0007(3)	0.0010(3)	0.0002(3)
O3	0.0099(4)	0.0085(4)	0.0077(4)	−0.0003(3)	0.0035(3)	0.0004(3)
O4	0.0107(4)	0.0061(4)	0.0113(4)	−0.0001(3)	0.0035(3)	0.0000(3)

TABLE 6b. Anisotropic displacement parameters U_{ij} (Å²) for reinhardbraunsite

Atom	U_{11}	U_{22}	U_{33}	U_{23}	U_{13}	U_{12}
Ca1	0.0092(2)	0.0078(2)	0.0089(2)	−0.00147(15)	0.00059(16)	−0.00105(15)
Ca2	0.00784(16)	0.00975(15)	0.00901(15)	−0.00043(10)	0.00321(12)	0.00078(11)
Ca3	0.00943(16)	0.00949(15)	0.00827(15)	0.00118(11)	0.00273(12)	0.00005(11)
Si1	0.0069(2)	0.00536(19)	0.00703(19)	−0.00004(14)	0.00194(15)	0.00015(15)
O1	0.0065(5)	0.0090(5)	0.0102(5)	−0.0002(4)	0.0022(4)	−0.0005(4)
O2	0.0089(5)	0.0090(5)	0.0083(5)	0.0001(4)	0.0015(4)	−0.0004(4)
O3	0.0103(5)	0.0090(5)	0.0079(5)	0.0000(4)	0.0033(4)	0.0003(4)
O4	0.0098(5)	0.0072(5)	0.0113(5)	−0.0002(4)	0.0029(4)	−0.0001(4)

TABLE 7. Selected interatomic distances (Å) for reinhardbraunsite and kumtyubeite

		Kumtyubeite	Reinhardbraunsite	Synth. OH*	Reinhardbr.†
Ca1	O1 ×2	2.3251(8)	2.3293(11)	2.335	2.328(2)
Ca1	O3 ×2	2.3821(8)	2.3853(11)	2.391	2.382(2)
Ca1	O4 ×2	2.4005(8)	2.3999(11)	2.404	2.401(2)
<Ca1-O>		2.3692	2.3715	2.377	2.370
Ca2	F5	2.2917(16)	2.266(5)		
Ca2	O5	2.359(4)	2.349(3)	2.325	2.295(5)
Ca2	O3	2.3113(9)	2.3119(11)	2.312	2.312(2)
Ca2	O1	2.3275(9)	2.3282(11)	2.323	2.324(2)
Ca2	O3	2.4090(9)	2.4062(12)	2.404	2.411(2)
Ca2	O2	2.4582(9)	2.4645(12)	2.470	2.457(2)
Ca2	O4	2.4802(9)	2.4909(12)	2.501	2.477(2)
<Ca2-O>		2.3909	2.3918	2.389	2.379
Ca3	O2	2.2745(8)	2.2908(11)	2.315	2.268(2)
Ca3	F5	2.2737(16)	2.271(5)		
Ca3	O5	2.358(4)	2.332(3)	2.316	2.279(5)
Ca3	F5	2.3026(16)	2.336(4)		
Ca3	O5	2.324(5)	2.330(2)	2.343	2.300(4)
Ca3	O2	2.3643(9)	2.3744(12)	2.379	2.369(2)
Ca3	O4	2.4060(9)	2.4111(11)	2.416	2.406(2)
Ca3	O1	2.4327(9)	2.4356(11)	2.443	2.434(2)
<Ca3-O>		2.3599	2.3623	2.369	2.343
Si1	O4	1.6225(9)	1.6218(11)	1.620	1.625(2)
Si1	O2	1.6424(9)	1.6455(12)	1.653	1.643(2)
Si1	O3	1.6456(9)	1.6455(12)	1.646	1.646(2)
Si1	O1	1.6471(9)	1.6489(12)	1.642	1.649(2)
<Si1-O>		1.6394	1.6404	1.6403	1.641
O5	H1	0.96(2)	0.94(2)		
H1	F5	1.92(2)	2.26(2)		
H1	O5	1.64(2)	1.90(2)		
O5	O5	2.594(9)	2.827(9)		
O5	F5	0.297(4)	0.377(13)		
O5	F5	2.880(4)	3.190(13)		
F5	F5	3.169(3)	3.56(2)		
O5	O2	3.300(2)	3.209(4)		
O5	H2		0.96(2)		
H2	O2		2.47(2)		

* $Ca_5(SiO_4)_2(OH)_2$ Kuznetsova et al. (1980).
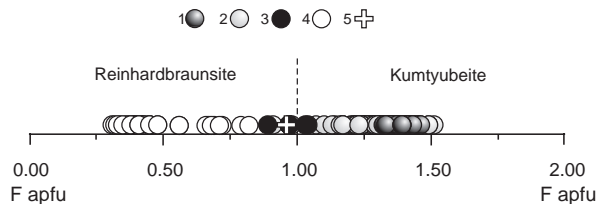† $Ca_5(SiO_4)_2(OH)F$ Kirfel et al. (1983).

FIGURE 6. Classification diagram of minerals of the reinhardbraunsite-kumtyubeite series: 1 = kumtyubeite from xenolith 1, holotype specimen, associated with rondorfite and spurrite; 2 = kumtyubeite from xenolith 1, associated with bultfonteinite; 3 = minerals of the reinhardbraunsite-kumtyubeite series, rims on spurrite grains; 4 = reinhardbraunsite from xenolith 1; 5 = analysis of holotype reinhardbraunsite, Eifel, Germany (Hamm and Hentschel 1983; Kirfel et al. 1983).

O···O distances in reinhardbraunsite-kumtyubeite are in general significantly longer than those in chondrodite. In chondrodite, H2 participates in a bifurcated hydrogen-bond system with O2 and O1 as acceptors. The O5-H2···O2 distance in "OH-chondrodite" is 2.88 Å and O5-H2···O1 is 3.01 Å (Yamamoto 1977; Lager et al. 2001), whereas the corresponding distances in reinhardbraunsite are 3.208 and 3.611 Å (this study). A special case is the O5-H1···O5′ distance, which is 3.07 Å in "OH-chondrodite" (Yamamoto 1977; Lager et al. 2001), but 2.827 Å in reinhardbraunsite (this study). "OH-chondrodite" displays IR absorptions characteristic of O-H stretching at 3527.2, 3562.0, and 3606.7 (weak) cm⁻¹ (Liu et al. 2003). For fluorine-dominant natural chondrodite, Frost et al. (2007b) report OH-specific Raman absorptions at 3561, 3570, and 3576 (shoulder) cm⁻¹. Thus, the closer range of hydrogen bonded O···O distances and stretching frequencies does not allow a definite band assignment.

One could also imagine a chondrodite or reinhardbraunsite structure with OH/F = 1 and H2 50% occupied but H1 vacant. However, this hypothetical model is in contradiction to all experimental studies based on direct localization of H or D by neutron or X-ray diffraction (e.g., Berry and James 2002; Friedrich et al. 2001; this study). Only if OH > 1 pfu does the H2 site become occupied (Yamamoto 1977; Lager et al. 2001; this study). The obvious preference of H1 over H2 has been discussed by several authors (e.g., Abbot et al. 1989; Berry and James 2002), however, without any convincing argument for the striking H1 selectivity.

Average Ca-O distances for Ca2 and Ca3 (Table 7) calculated from our reinhardbraunsite structure refinement are significantly longer than those cited by Kirfel et al. (1983). Kirfel et al. (1983) reported average O/F distances, which are shorter than pure Ca-O of our O/F sub-site model.

In reinhardbraunsite, kumtyubeite (this paper), and "OH-chondrodite" (Yamamoto 1977), the sequence of angular distortions for octahedra is M1O₆ > M2O₆ > M3O₆. Differences in bond-length distortion are much less pronounced, and corresponding octahedra in reinhardbraunsite, kumtyubeite, and chondrodite have similar bond-length distortions. However, if the bond-angle variance (Robinson et al. 1971) is applied as a measure of polyhedral distortion (Table 8), variances for corresponding octahedra in reinhardbraunsite and kumtyubeite are almost twice as high as those in chondrodite. On the other hand, SiO₄ tetrahedra in reinhardbraunsite and kumtyubeite are

(Libowitzky 1999), the low-frequency band at ca. 3480 cm⁻¹ in the reinhardbraunsite Raman spectrum (Fig. 3) is related to O5-H1···O5′, whereas the weaker hydrogen bonds O5-H1···F5′ and O5-H2···O2 are related to the bands near 3550–3560 cm⁻¹. In kumtyubeite, the only hydrogen bond system is O5-H1···F5′ with an O5···F5′ distance of 2.880 Å. The corresponding Raman and FTIR spectra (Figs. 2 and 3) display a set of closely spaced absorptions around 3553 cm⁻¹, which must be assigned to the hydrogen bond O5-H1···F5′.

If the correlation between O-H stretching frequencies and O-H···O hydrogen bond length (Libowitzky 1999) is assumed to be qualitatively correct even for a rather narrow range of O···O distances between ca. 2.8 and 3.3 Å, the characteristic IR and Raman absorption at ca. 3480 cm⁻¹, found only in the OH-dominant reinhardbraunsite but not in F-dominant kumtyubeite, is caused by the short O5-H1···O5′ hydrogen bond system (2.827 Å) but not by O5-H2···O2 (3.209 Å), as one might expect at first glance. The O5-H1···O5′ bond system is also unique to reinhardbraunsite, whereas kumtyubeite has a corresponding O5-H1···F5′ system, which is considerably weaker, as evidenced by the increased absorption frequency near 3550–3560 cm⁻¹.

However, this assignment is only suggested for the reinhardbraunsite–kumtyubeite series, but not, e.g., for the isotypic Mg-rich members chondrodite and synthetic "OH-chondrodite." Humite-group minerals are based on a hexagonal closest-packing of anions. Due to the smaller radius of Mg compared to Ca,

TABLE 8. Bond-angle variance for MO_6 octahedra and SiO_4 tetrahedra in reinhardbraunsite, kumtyubeite (this study), and "OH-chondrodite" (Yamamoto 1977)

Polyhedron	Reinhardbraunsite	Kumtyubeite	"OH-chondrodite"
M1 octahedron	$(216°)^2$	$(216°)^2$	$(106°)^2$
M2 octahedron	$(159°)^2$	$(172°)^2$	$(76°)^2$
M3 octahedron	$(119°)^2$	$(120°)^2$	$(71°)^2$
Si1 tetrahedron	$(22°)^2$	$(22°)^2$	$(45°)^2$

less distorted in their O-T-O angles than those in chondrodite (Table 8). The different distortion behavior in Ca and Mg minerals is related to a cation-size effect (Ca vs. Mg). Within a larger CaO_6 octahedron oxygen atoms have a higher flexibility in their arrangement without coming too close to each other, whereas the chondrodite structure (Yamamoto 1977) is much closer to a hexagonal closest-packed anion (O,F) arrangement giving rise to more ideal octahedral geometry. As the CaO_6 moieties are the flexible links in the reinhardbraunsite and kumtyubeite structure, SiO_4 tetrahedra are less distorted than in chondrodite.

DISCUSSION

About 150 compositions from microprobe analyses of reinhardbraunsite-kumtyubeite solid-solution members from skarn xenoliths of the Upper Chegem volcanic structure are plotted on a classification diagram (Fig. 6). They form a continuous solid-solution series with common crystal-chemical formula $Ca_5(SiO_4)_2(OH,F)_2$ from $F/(F + OH) \approx 0.15$ (maximally hydrated reinhardbraunsite) to $F/(F + OH) \approx 0.75$ (maximally fluorinated kumtyubeite). The absence of kumtyubeite with higher F content up to $F/(F + OH) = 1$ may be explained by the stabilizing role of hydrogen bonds in humite-group structures (Berry and James 2002). Available data allow us to ascertain a minimal OH amount near 0.25 pfu necessary for kumtyubeite formation. For this minimum OH concentration, the proton participates only in the hydrogen bond O5-H1···F5′. Kumtyubeite crystallization is connected with the early stage of alteration of primary minerals (larnite and spurrite) in high-temperature skarns, formed according to Korzhinsky (1940) at the larnite-mervinite depth facies, corresponding to the *P-T* conditions of the sanidinite facies of metamorphism (Zharikov and Shmulovich 1969; Pertsev 1977; Korzhinski 1940; Gazeev et al. 2006; Callegari and Pertsev 2007; Galuskin et al. 2008). In Caucasian xenoliths, kumtyubeite occurs in mineral associations characteristic of higher temperature than those where reinhardbraunsite formed. Kumtyubeite and reinhardbraunsite replace "Ca-humites," which, in turn, formed at the expense of larnite and spurrite. The most fluorine-rich kumtyubeite formed in the internal part of skarns together with cuspidine $Ca_4Si_2O_7[F_{1.9}(OH)_{0.1}]$, which replaces larnite at the contact with the ignimbrite.

REFERENCES CITED

Abbot, R.N., Burnham, C.W., and Post, J.E. (1989) Hydrogen in humite-group minerals: Structure-energy calculations. American Mineralogist, 74, 1300–1306.
Barker, D.S. and Nixon, P.H. (1989) High-Ca, low-alkali carbonatite volcanism at Fort Portal, Uganda. Contributions to Mineralogy and Petrology, 103, 166–177.
Berry, A.J. and James, M. (2001) Refinement of hydrogen position in synthetic hydroxyl-clinohumite by powder neutron diffraction. American Mineralogist, 86, 181–184.
——— (2002) Refinement of hydrogen position in natural chondrodite by powder neutron diffraction: Implication for the stability of humite minerals. Mineralogical Magazine, 66, 441–449.
Bruker (1999) SMART and SAINT-Plus. Versions 6.01. Bruker AXS Inc., Madison, Wisconsin.
Callegari, E. and Pertsev, N. (2007) Contact Metamorphic and Associated Rocks. Metamorphic rocks. A classification and glossary of terms, p. 69–81. Cambridge University Press, U.K.
Chesnokov, B.V., Bazhenova, L.F., Bushmakin, A.F., Vilisov, V.A., Kretser, Yu.L., and Nishanbaev, T.P. (1993) New minerals from burned dumps at Chelyabinsk coal basin (fourth report). Ural mineralogical collection of scientific papers, UIF "Nauka," Ekaterinburg, 1, 15–18.
Friedrich, A., Lager, G.A., Kunz, M., Chakoumakos, B.C., Smyth, J.R., and Schultz, A.J. (2001) Temperature-dependent single-crystal neutron diffraction study of natural chondrodite and clinohumites. American Mineralogist, 86, 981–989.
Frost, R.L., Palmer, S.J., and Reddy, B.J. (2007a) Near-infrared and mid-IR spectroscopy of selected humite minerals. Vibrational Spectroscopy, 44, 154–161.
Frost, R.L., Palmer, S.J., Bouzaid, J.M., and Reddy, B.J. (2007b) A Raman spectroscopic study of humite minerals. Journal of Raman Spectroscopy, 38, 68–77.
Galuskin, E.V., Gazeev, V.M., Armbruster, Th., Zadov, A.E., Galuskina, I.O., Pertsev, N.N., Dzierżanowski, P., Kadiyski, M., Gurbanov, A.G., Wrzalik, R., and Winiarski, A. (2008) Lakargiite CaZrO₃: A new mineral of the perovskite group from the North Caucasus, Kabardino-Balkaria, Russia. American Mineralogist, 93, 1903–1910.
Ganiev, R.M., Kharitonov, Yu.A., Ilyukhin, V.V., and Belov, N.V. (1969) The crystal structure of calcium chondrodite Ca₅(SiO₄)₂(OH)₂ = Ca(OH)₂(Ca₂SiO₄)₂. Doklady Akademii Nauk SSSR, 188, 1281–1283 (in Russian).
Gazeev, V.M., Zadov, A.E., Gurbanov, A.G., Pertsev, N.N., Mokhov, A.V., and Dokuchaev, A.Ya. (2006) Rare minerals from Verkhniechegemskaya caldera (in xenoliths of skarned limestone). Vestnik Vladikavkazskogo Nauchnogo Centra, 6, 18–27 (in Russian).
Gekimyants, V.M., Sokolova, E.V., Spiridonov, E.M., Ferraris, G., Chukanov, N.V., Prencipe, M., Avdonin, V.N., and Polenov, V.N. (1999) Hydroxylclinohumite Mg₉(SiO₄)₄(OH,F)₂—a new mineral of the humite group. Zapiski Vsesuyuznogo Mineralogicheskogo Obschestva, 5, 64–70 (in Russian).
Gibbs, J.V., Ribbe, P.H., and Anderson, C.P. (1970) The crystal structures of the humite minerals. II. Chondrodite. American Mineralogist, 55, 1182–1194.
Gutt, W. and Osborne, G. J. (1966) The system 2CaO.SiO₂-CaF₂. Transactions of the British Ceramic Society, 65, 521–534.
Hamm, H.M. and Hentschel, G. (1983) Reinhardbraunsite, Ca₅(SiO₄)₃(OH,F)₂, a new mineral—the natural equivalent of synthetic "calcio-chondrite." Neues Jahrbuch für Mineralogie, Monatshefte, 119–129.
Jones, N.W., Ribbe, P.H., and Gibbs, G.V. (1969) Crystal structure of the humite minerals. American Mineralogist, 54, 391–411.
Karimova, O., Zadov, A., Gazeev, V., and Ivanova, A. (2008) New data on reinhardbraunsite: New locality, properties and structure refinement. Proceedings of the International Geological Congress, 6–14 of August, Oslo.
Kirfel, A., Hamm, H.M., and Will, G. (1983) The crystal structure of reinhardbraunsite, Ca₅(SiO₄)₂(OH,F)₂, a new mineral of the calcio-chondrite type. Tschermaks Mineralogische und Petrographische Mitteilungen, 31, 137–150.
Korzhinsky, D.S. (1940) Factors of mineral equilibria and mineralogical facies of depths. Transactions of Institute of Geological Sciences, 12, 99 p. (in Russian).
Kraus, W. and Nolze, G. (1996) POWDER CELL—a program for the representation and manipulation of crystal structures and calculation of the resulting X-ray powder patterns. Journal of Applied Crystallography, 29, 301–303.
Kuznetsova, T.P., Nevskii, N.N., Ilyukhin, V.V., and Belov, N.V. (1980) Refinement of the crystal structure of calcium chondrodite Ca₅(SiO₄)₂(OH)₂ = Ca(OH)₂(Ca₂SiO₄)₂. Soviet Physics Crystallography, 25, 91–92.
Lager, G.A., Armbruster, T., and Faber, J. (1987) Neutron and X-ray diffraction study of hydrogarnet Ca₃Al₂(O₄H₄)₃. American Mineralogist, 72, 756–765.
Lager, G.A., Ulmer, P., Miletich, R., and Marshall, W.G. (2001) O-D···O bond in OD-chondrodite. American Mineralogist, 86, 176–180.
Libowitzky, E. (1999) Correlation of O-H stretching frequencies and O-H···O hydrogen bond lengths in minerals. Monatshefte für Chemie, 130, 1047–1059.
Liu, Z., Lager, G.A., Hemley, R.J., and Ross, N.L. (2003) Synchrotron infrared spectroscopy of OH-chondrodite and OH-clinohumite. American Mineralogist, 88, 1412–1415.
Ottolini, L., Cámara, F., and Bigi, S. (2000) An investigation of matrix effects in the analysis of fluorine in humite-group minerals by EMPA, SIMS, and SREF. American Mineralogist, 85, 89–102.
Pertsev, N.N. (1977) High Temperature Metamorphism and Metasomatism of

Carbonate Rocks, 255 p. Nauka, Moscow (in Russian).

Prasad, P.S.R. and Sarma, L.P. (2004) A near-infrared spectroscopic study of hydroxyl in natural chondrodite. American Mineralogist, 89, 1056–1060.

Ribbe, P.H. and Gibbs, G.V. (1971) Crystal structure of the humite minerals: III. Mg/Fe ordering in humite and its relation to other ferromagnesian silicates. American Mineralogist, 56, 1155–1173.

Robinson, K., Gibbs, G.V., and Ribbe, P.H. (1971) Quadratic elongation: A quantitative measure of distortion in coordination polyhedra. Science, 172, 567–570.

Shannon, R.D. (1976) Revised ionic radii and systematic studies of interatomic distances in halides and chalcogenides. Acta Crystallographica, A32, 751–767.

Sheldrick, G.M. (1996) SADABS. University of Göttingen, Germany.

——— (1997) SHELXL-97. A program for crystal structure refinement. University of Göttingen, Germany.

Sokol, E.V., Novikov, I.S., Vapnik, Y., and Sharygin, V.V. (2007) Gas fire from mud volcanoes as a trigger for the appearance of high-temperature pyrometamorphic rocks of the Hatrurim formation (Dead Sea area). Doklady Earth Sciences, 413A, 474–480.

Strunz, H. and Nickel, E. (2001) Strunz Mineralogical Tables, 9th edition, 870 p.

Schweizerbart'scheVerlagsbuchhandlung, Stuttgart.

Taylor, H.F.W. (1997) Cement Chemistry, second edition, 459 p. Thomas Telford, London.

Thompson, J.B. (1978) Biopyriboles and polysomatic series. American Mineralogist, 63, 239–249.

Watanabe, T., Fukuyama, H., and Nagata, K. (2002) Stability of cuspidine (3CaO 2SiO$_2$ CaF$_2$) and phase relations in the CaO-SiO$_2$-CaF$_2$ system. ISIJ International, 42, 489–497.

Yamamoto, K. (1977) The crystal structure of hydroxyl-chondrodite. Acta Crystallographica, B33, 1481–1485.

Zharikov, V.A. and Shmulovich, K.I. (1969) High-temperature mineral equilibrium in the system CaO-SiO$_2$-CO$_2$. Geochemistry, 9, 1039–1056 (in Russian).